The Boson Peak of Amyloid Fibrils: Probing the Softness of Protein Aggregates by Inelastic Neutron Scattering

ARTICLE *in* THE JOURNAL OF PHYSICAL CHEMISTRY B · FEBRUARY 2014

Impact Factor: 3.3 · DOI: 10.1021/jp412277y · Source: PubMed

7 AUTHORS, INCLUDING:

Giorgio Schirò
French National Centre for Scientific Research
33 PUBLICATIONS **374** CITATIONS
SEE PROFILE

Valeria Vetri
Università degli Studi di Palermo
39 PUBLICATIONS **769** CITATIONS
SEE PROFILE

Maurizio Leone
Università degli Studi di Palermo
154 PUBLICATIONS **2,411** CITATIONS
SEE PROFILE

Antonio Cupane
Università degli Studi di Palermo
137 PUBLICATIONS **1,910** CITATIONS
SEE PROFILE

THE JOURNAL OF PHYSICAL CHEMISTRY B

Article

pubs.acs.org/JPCB

The Boson Peak of Amyloid Fibrils: Probing the Softness of Protein Aggregates by Inelastic Neutron Scattering

G. Schirò,*[,†,⊥] V. Vetri,[†] C.B. Andersen,[‡] F. Natali,[§] M.M. Koza,[∥] M. Leone,[†] and A. Cupane[†]

[†]Dipartimento di Fisica e Chimica, Università di Palermo, 90136 Palermo, Italy

[‡]Department of Diabetes Biophysics, Novo Nordisk A/S, Novo Nordisk Park, DK-2760 Måløv, Denmark

[§]CNR-IOM, c/o Institut Laue Langevin, Grenoble, France

[∥]Institut Laue Langevin, Grenoble, France

Supporting Information

ABSTRACT: Proteins and polypeptides are characterized by low-frequency vibrations in the terahertz regime responsible for the so-called "boson peak". The shape and position of this peak are related to the mechanical properties of peptide chains. Amyloid fibrils are ordered macromolecular assemblies, spontaneously formed in nature, characterized by unique biological and nanomechanical properties. In this work, we investigate the effects of the amyloid state and its polymorphism on the boson peak. We used inelastic neutron scattering to probe low-frequency vibrations of the glucagon polypeptide in the native state and in two different amyloid morphologies in both dry and hydrated sample states. The data show that amyloid fibril formation and hydration state affect the softness of the polypeptide not only by changing the distribution of vibrational modes but also, and most significantly, the dissipative mechanisms of collective low-frequency vibrations provided by water−protein and protein−protein interactions. We show how the morphology of the fibril is able to tune these effects. Atomic fluctuations were also measured by elastic neutron scattering. The data confirm that any effect of protein aggregation on fluctuation amplitudes is essentially due to changes in surface exposure to hydration water. The results demonstrate the importance of protein−protein and protein−water interactions in the dynamics and mechanics of amyloid fibrils.

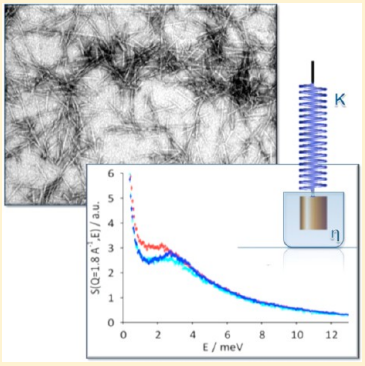

INTRODUCTION

Many proteins are characterized by an intrinsic propensity to form ordered supramolecular assemblies, called amyloid fibrils, characterized by a double-pleated beta-sheet that forms the spine of these extended structures. Fibrils are formed under a wide range of conditions and by a diversity of proteins and peptides. Moreover, amyloid fibrils are considered to be at the root of degenerative diseases;[1] they present a great challenge to drug discovery and formulation[2] and have a functional role in many living species.[3] The intrinsic and tunable diversity of fibril structures gives a wide range of opportunities in designing new nanomaterials.[4,5] Due to their high stability and conductivity properties, they may have potential applications as nanowires or they could assemble into 3D structures that can be used as scaffolds for nanotechnological engineering. Moreover, their surface can be easily functionalized to tailor their chemical interactions. Understanding the role of fibrils in the function/misfunction of biological systems and their potential use as self-assembled natural nanomaterials requires a detailed knowledge of their physical and mechanical properties. It was recently shown that amyloid fibrils are characterized by extraordinary mechanical properties.[6,7] For example, insulin fibrils were shown to have strength comparable to that of steel and a mechanical stiffness comparable to that of silk.[6] The origin of these properties appears to be related to the way protein molecules interact when forming amyloid aggregates, i.e., the structural hierarchy and protofilament packing, but also to fibril length and thickness.

Fibrils are typically formed from a lateral arrangement of a number of protofilaments, which leads to the concept of fibrillar polymorphism. It has been shown that polymorphism is perpetuated at all structural levels all the way to the individual protofilaments, which exhibit differences in side chain packing, hydrogen bond networks, as well as the secondary and tertiary structure.[8−10] Although polymorphism is widely observed in amyloid fibrils, a detailed understanding of its role and the effect on fibril properties is still incomplete.

Various methods—including atomic force microscopy (AFM), spectroscopy, and quartz crystal oscillator—have been applied to investigate amyloid mechanical properties.[6,11] AFM can be used to probe the deformation of polypeptide chains involved in the amyloid structure by bringing them out of their equilibrium state by means of an external force in both linear and nonlinear regimes. However, the response relaxation of a system from a nonequilibrium state to the equilibrium state is related to its fluctuation properties at the equilibrium. Indeed,

Received: December 16, 2013
Revised: February 18, 2014
Published: February 25, 2014

the elastic properties of a polymeric system depend on the interactions stabilizing the structure: these interactions determine the relaxation behavior and the time/space scale of low-frequency structural vibrations. Here we pursue an equilibrium approach where the effect of the amyloid state on the visco-elastic properties of proteins is studied by probing the low-frequency vibrations of atomic nuclei occurring in the terahertz (THz) dynamical range by inelastic neutron scattering. Neutron scattering from D_2O-hydrated protein powders gives information on the dynamics of nonexchangeable hydrogen atoms due to the large incoherent cross section of hydrogen nuclei with respect to the other nuclei present in proteins. The nonexchangeable hydrogen atoms are essentially from the CH, CH_2, and CH_3 groups, which are uniformly distributed over the protein structure. Neutron spectra are composed by the central elastic line (neutrons scattered without energy exchange, i.e., from nuclei not moving on the time scale set by the resolution of the spectrometers), the quasi-elastic broadening (neutrons scattered with energy exchange approximately <1 meV, due to diffusive motions of scatterers nuclei), and the inelastic part (energy exchange approximately >1 meV, due to vibrational modes). The spectral shape of the inelastic response is related to vibrational density of intra- and intermolecular modes and hence to the forces acting in proteins and their surroundings. It has been experimentally proven—and even predicted by normal-mode analysis and molecular dynamics simulations—that proteins are characterized by delocalized collective vibrations at about 3 meV ($\approx$24 cm^{-1} or $\approx$0.7 THz),[12−15] which can be damped by the friction due to the water−protein interactions but also to inter- and intraprotein interactions.[16,17] The broad band corresponding to these vibrations has been measured by inelastic neutron scattering and Raman spectroscopy, and has been dubbed the boson peak. Although several models have been proposed to explain the origin and the features of the boson peak in polymers and polypeptides (see, e.g., ref 13 and references therein), it is widely accepted that they are directly related to the viscoelastic behavior of protein structures and surroundings. The boson peak of protein powders usually shows a frequency shift and a shape change as a function of hydration level: the spectrum appears to get softer (red-shifted) in the dry powders and harder (blue-shifted) in the hydrated ones.[18] No significant protein chemical/structural changes are expected when changing hydration level, except for a propensity to increase the content of β-sheet secondary structures[19] on drying. Since β-structures are thought to be stiffer than any other secondary structure motifs,[20−22] one would expect a blue shift in dry samples. The only way to explain the experimentally measured red shift is to attribute the change in the boson peak shape to a variation of dissipative mechanisms provided by protein−water and protein−protein interactions. Indeed, the presence of the water matrix in hydrated samples provides a dissipative bath for protein vibrations via hydrogen bond and electrostatic interactions, which is able to suppress vibrational modes and thus change the boson peak shape. This means that the "effective" softness of proteins, which is revealed by the shape and position of the boson peak, depends not only on the "intrinsic" normal-mode distribution (determined by the intramolecular forces) but also on protein−water and protein−protein interactions (determining the dissipative mechanism). This idea has been proposed by W. Doster and co-workers previously.[18] Their quantitative approach to describe the damping mechanism was based on the formalism of the mode-coupling theory.[23] Here we used a similar approach to quantitatively interpret our experimental results, as fully described in the next section. Other models proposed in the literature to predict the boson peak shape in proteins have here been discarded. For example, the quasi-continuum model[24] failed in its prediction of a close relationship between protein native state and low-frequency motions, so that the fundamental frequencies should disappear upon denaturation. This prediction was recently questioned by a study on the boson peak in the absence of peptide bond.[25] Another model, the elastic global model,[26] failed in predicting a relationship of inverse proportionality between the boson peak frequency and the radius of the protein. Indeed, an extensive study on different proteins[21] clearly showed that the boson peak position is not related to the size of the protein.

In order to analyze the effect of supramolecular organization and polymorphism on this class of protein motions, glucagon was selected as a model system. Glucagon is a small hormone peptide comprised of 29 amino acids involved in the regulation of blood sugar levels and used therapeutically in cases of hypoglycemia.[27] Glucagon fibril formation was first reported in 1968,[28] and it is today often used as a model for fibril formation and structural polymorphism.[29,30] When glucagon fibrillates, it forms a number of unique fibril morphologies, which show a remarkable dependence on the external conditions at which they were formed (e.g., temperature, stress, formulation conditions). This essentially makes it possible to produce a specific morphology as confirmed in a number of studies.[31−35]

In this study, we focused on two well-characterized morphologies: glucagon fibrils formed at acidic pH and low concentration (0.25 g/L) which consist of two or more filaments with a regular twist (twisted fibrils) and fibrils formed at high concentration (8 g/L) consisting of two straight filaments (straight fibrils). We used the position and shape of the boson peak as a marker of the viscoelastic properties of the glucagon peptide in the twisted and straight fibril morphology and compared them with lyophilized, native glucagon. Results presented here are relevant in two aspects. First of all, they confirm that the shape of the boson peak spectrum is determined not only by the intrinsic vibrational density of states but also by the dissipation mechanism of vibrational modes. Second, they highlight the role of polymorphism and surface hydration in modulating the mechanical properties of amyloid fibrils.

MATERIALS AND METHODS

Samples. Pharmaceutical grade glucagon lyophilized powder (Novo Nordisk A/S, Bagsværd, Denmark) was fibrillated into two distinct morphologies denoted twisted and straight based on a protocol published previously.[32] Briefly, glucagon was dissolved in 0.22 μm sterile-filtered glycine/HCl buffer adjusted to pH 2.5 and the dissolved sample then centrifuged to remove undissolved powder and aggregates. To obtain mature twisted and straight fibrils, glucagon samples were incubated at 25 °C for 48 h at 0.25 and 8 g/L concentration, respectively. Peptide concentration was estimated by UV absorption spectroscopy at 280 nm using a theoretical molar extinction coefficient of 8250 M^{-1} cm^{-1}.

Fibril formation was verified by means of a thioflavin T (ThT) assay, and the distinct fibril morphologies were verified by circular dichroism (CD) and Fourier transform infrared (FTIR) spectroscopy (data not shown). Fibril samples were then dialyzed against H_2O to remove buffer components.

dx.doi.org/10.1021/jp412277y | J. Phys. Chem. B 2014, 118, 2913−2923

Samples were concentrated by a factor of 10 and washed in D_2O using a nitrogen pressurized filtering system with a 30 kDa cutoff (Amicon, US). At this step, control measurements were also performed to verify the sample aggregation state. Samples were then equilibrated in D_2O for 12 h and subsequently lyophilized. Lyophilized samples were dried for about 1 day under vacuum until the sample weight had stabilized and the resulting powders were considered as dry samples ($h = 0$ where h is defined as grams of D_2O per gram of dry protein). Suitable aliquots of the dry powders were then held in D_2O atmosphere and left to reach a hydration level of $h = 0.15$ determined by measuring the mass change. The choice of the hydration level is aimed to ensure that the scattering signal essentially arises from nonexchangeable H atoms of protein while the water signal is negligible. In order to get a homogeneous hydration, the samples were left to equilibrate for about 10 days before measurements. Straight and twisted fibril samples were prepared identically in parallel, and about 750 mg of glucagon was required for these experiments. Fibrillation of glucagon generally goes to completion with only a low percentage of monomers present in the fibrillated samples.

Experiments. FTIR measurements were performed on glucagon powders dissolved in D_2O with a Bruker (Ettlingen, Germany) Vertex 70 FTIR single-beam spectrometer equipped with a MIR light source and a DLATGS pyroelectric detector. Each measurement reported is an average of 200 spectra in the 400−4000 cm^{-1} range with a spectral resolution of 2 cm^{-1}.

Transmission electron microscopy samples were prepared on a 300-mesh Cu grid with a carbon film. Samples in the powder state prepared as described above were rediluted in Milli-Q water with uranyl acetate, and finally analyzed on a MORGANI FP 5005 TEM system with an Image Analysis 2003 soft imaging system from FEI Company (Oregon, USA).

ThT fluorescence spectra (40 μM ThT, excitation wavelength $\lambda_{ex} = 440$ nm) were measured in the range 450−650 nm on a JASCO (Tokyo, Japan) FP-8500 spectrofluorimeter equipped with a Peltier thermostat in a quartz cuvette with 1 cm light path. CD measurements were performed in the far-UV region on a JASCO J-715 spectropolarimeter equipped with a JASCO PCT 348WI temperature controller at 50 nm/min scan speed, 1 nm bandwidth, and 0.1 nm data pitch.

Inelastic neutron scattering experiments were performed at the time-focusing time-of-flight spectrometer IN6 (Institut Laue-Langevin, Grenoble, France) with an incident wavelength of $\lambda = 5.1$ Å and an energy resolution of 70 μeV fwhm. The setting allows access to the momentum transfer range 0.3 $Å^{-1} < Q < 2$ $Å^{-1}$. The spectra were collected at $T = 150$ K where quasielastic contributions are negligible.

Elastic neutron scattering temperature scans (20−300 K) were performed at the thermal backscattering spectrometer IN13 (incident wavelength $\lambda = 2.23$ Å; Institut Laue-Langevin, Grenoble, France) that allows access to a large momentum transfer range 0.2 $Å^{-1} < Q < 4.9$ $Å^{-1}$ with an almost Q-independent energy resolution of 8 μeV fwhm. The elastic energy value was kept fixed within 3 μeV of accepted tolerance. The elastically scattered intensity was corrected for the empty cell contribution and normalized with respect to the lowest temperature scan ($T = 20$ K) to compensate for spurious background contributions and detector efficiency.

In order to avoid corrections from multiple scattering contributions, in all the experiments (both on IN13 and IN6), the cell thickness and geometry were properly chosen to optimize the neutron transmission through the sample. A typical 0.9 transmission was obtained using a flat 0.4 mm thick aluminum sample holder.

Data Analysis. The inelastic spectra $S(Q, E)$, where E denotes the exchanged energy at the momentum transfer, $Q = 1.8$ $Å^{-1}$, reported here, were obtained by binning all the measured spectra in the interval 1.6 $Å^{-1} < Q < 2.0$ $Å^{-1}$. In view of the relation between energy and momentum transfer ranges in a time-of-flight spectrometer, the choice of this Q region allows to explore the largest energy range accessible. The spectra were then normalized for the elastic peak intensity.

As described in the Introduction, we used a quantitative approach proposed by W. Doster and co-workers[18] to describe the water-damping mechanism. The introduction of a dissipative mechanism makes it possible to explain the experimentally observed change of boson peak shape which is otherwise apparently at odds with the increase in β-structures observed in the dry protein powders. This approach is based on the formalism of the mode-coupling theory.[23] We define the dynamic structure factor $S(Q, E)$ corresponding to each vibrational mode of energy ε as the imaginary part of the product $S(Q)\Psi(Q, E)$, where $S(Q)$ is the static structure factor and $\Psi(Q, E)$ is

$$\Psi(Q, E) = -\frac{E + \varepsilon^2 M(Q, E)}{E^2 - \varepsilon^2 + E\varepsilon^2 M(Q, E)} \quad (1)$$

$M(Q, E) = i\gamma(Q) + \mu(Q, E)$ is a generalized friction function composed of a Newtonian term $\gamma(Q)$ and a relaxation term that can be derived from the Maxwell model for a viscoelastic liquid system $\mu(E) = -F/(E + i/\tau)$. The F and τ parameters (i.e., the amplitude and the relaxation time of the Maxwell term, respectively) define the way the modes are damped by the coupling with a dissipative bath: the larger F is and the smaller τ is, the more effective is the dissipative mechanism. The function $\Psi(Q, E)$ refers to a single mode of energy ε, so it must be convoluted with a distribution function $\Gamma(\varepsilon)$ (where $\Gamma(\varepsilon)\,d\varepsilon$ is the number of modes with energy between ε and $\varepsilon + d\varepsilon$), which is usually defined as vibrational density of states (V-DOS). There are several models proposed in the literature to calculate the distribution function for amorphous systems, and here we choose an asymmetric log-normal distribution:

$$\Gamma(\varepsilon) = \frac{\alpha}{\varepsilon} \exp\left[\frac{-(\Theta - \ln \varepsilon)^2}{2\rho^2}\right] \quad (2)$$

where α is a normalization factor, while Θ and ρ are the center and the width of the distribution, respectively.[36] The function used to analyze the experimental spectra at $Q = 1.8$ $Å^{-1}$ then has the following form:

$$S_{exp}(E, Q = 1.8) = a \int \Gamma(\varepsilon)\mathcal{I}[\Psi(E, \varepsilon)]\,d\varepsilon + b \quad (3)$$

where $\mathcal{I}$ is the imaginary part operator, a is a global scale factor, and b is a constant term which accounts for the flat contribution of the fast diffusive motions plus the instrumental background. The integration is performed in the $[0, \infty]$ energy interval. Note that the contribution from the tails of the elastic peak is not considered, since it is negligible in the explored energy range. Inelastic spectra were analyzed with a FORTRAN 95 program written for this purpose and based on the *Minuit* minimization routine released by the CERN computing group (lcgapp.cern.ch/project/cls/work-packages/mathlibs/minuit/index.html).

dx.doi.org/10.1021/jp412277y | J. Phys. Chem. B 2014, 118, 2913−2923

We calculated the mean square displacements msd $\equiv \langle \Delta u^2 \rangle / 6$ from the elastic scattered intensity $S(Q, T, E = 0)$ with the Gaussian approximation:[37]

$$-\ln\left[\frac{S(Q, T, E=0)}{S(Q, T=20\ \mathrm{K}, E=0)}\right] = \frac{\langle u^2(T)\rangle - \langle u^2(20\ \mathrm{K})\rangle}{6}Q^2 = \frac{\langle \Delta u^2(T)\rangle}{6}Q^2 \quad (4)$$

RESULTS AND DISCUSSION

Sample Characterization. It is well established that, at acidic pH, glucagon is prone to form amyloid fibrils and that the fibril morphologies are highly dependent on the sample conditions.[34] In particular, by only adjusting the peptide concentration, glucagon may form twisted or straight fibrils at 0.25 and 8 g/L, respectively.[32] Twisted fibrils consist of two or more protofilaments intertwined with a regular periodicity, while straight fibrils consist of two straight, adjacent protofilaments.[32,33]

Morphological differences were found to be perpetuated at all structural levels and included the amino acid sequences in the beta-sheet fibril core protected from proteolytic digest, the secondary structure elements evident in CD and FTIR spectroscopy, the chromophore alignment along the fibril axis as probed by linear dichroism, as well as the overall fibril superstructure visualized by TEM.[33]

The aim of this work is to measure the boson peak of amyloid fibrils and to investigate the effects of polymorphism mentioned above. To do this, we produced amyloid glucagon fibrils using the protocol described in Andersen et al.[33] but modified to obtain hydrated powder samples. The same approach was used in a previous work to produce samples with conserved amyloid state.[38] To verify that freeze-drying and sample rehydration do not affect the morphology and the molecular properties, the samples were analyzed by TEM and FTIR and compared to previously reported data. In Figure 1, FTIR absorption spectra in the amide I′ region from fibril powder samples redissolved in D_2O after neutron scattering experiments are shown with native glucagon included for comparison (red dashed line). The straight fibril morphology spectrum (cyan line) has an intense absorption peak at 1620 cm^{-1}, typical for the very strong intermolecular hydrogen bonds found in amyloid β-sheet, and a small shoulder attributable to the presence of α-helices is also evident at higher wavenumbers.[33] The twisted fibril morphology spectrum (blue line) has two peaks at 1626 and 1632 cm^{-1}, a shoulder at 1645 cm^{-1}, and the beta turn peak at 1664 cm^{-1} as previously found for this morphology.[33] These data confirm that the samples retain their secondary structure after freeze-drying and hydration procedures.[38] The FTIR results also reveal that the backbone structure in the protofilaments strongly depends on the morphology with the hydrogen bonds in the twisted morphology being weaker than those of the straight morphology, as indicated by the intermolecular β-sheet peak being shifted to lower wavenumbers in straight fibril samples.[33]

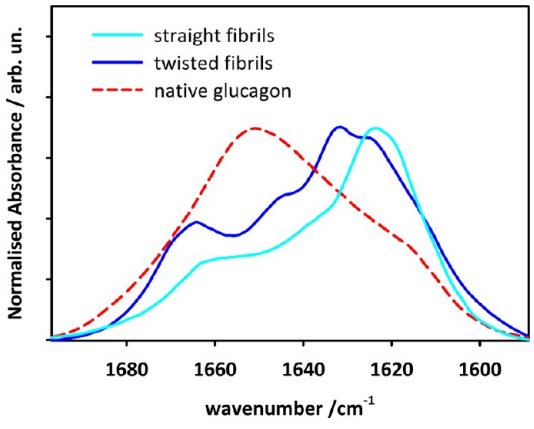

Figure 1. Amide I′ absorption spectra of glucagon powder samples redissolved in D_2O, straight fibrils (cyan line), twisted fibrils (blue line), and native glucagon (red dashed line).[33] The spectra of fibrils show significant morphology-dependent differences at wave numbers pertaining to extended beta-strand structures.

Figure 2 shows TEM pictures of fibrillated glucagon samples after the freeze-drying procedure. In panel a, fibrils formed at low peptide concentration are found to exhibit the same twisted morphology reported previously, while the fibrils formed at high concentration in panel b are straight as expected.[32,33] We do note, however, that the freeze-drying procedure seems to fracture the fibrils into shorter pieces (about 200 nm after freeze-drying vs >1 μm before[33]).

Inelastic Neutron Scattering. In Figure 3, we report the dynamic structure factors $S(E)$—obtained from normalized inelastic scans at T = 150 K and Q = 1.8 $Å^{-1}$—of monomeric and fibrillated glucagon samples in the dry and hydrated states (panels a and b, respectively). The measurements were performed at 150 K in order to minimize the contribution of quasi-elastic broadening. As can be seen, a broad boson peak centered at about 3 meV (~0.7 THz) is observed for all samples, likely due to low frequency vibrational/librational protein internal motions. For the fibril samples, contributions from collective bending/torsional/axial stretching normal modes falling in the frequency range 0.1−1 THz (as predicted, e.g., by Buehler and co-workers[39] and Eom and co-workers[40]) cannot be excluded.

The effect of the amyloid state on the boson peak is highlighted in panels c and d, where we report the difference spectra between native and fibrillated samples in both the dry and hydrated state. In dry samples, the amyloid state is characterized by a depression of low-frequency scattering and by an apparent shift of the boson peak toward higher energies with respect to the native state. The effect depends on fibrillar morphology and is smaller for twisted than for straight fibrils. The effect of hydration on homologous samples is highlighted in Supporting Information (Figures S1 and S2). Hydrated samples are characterized by depressed scattering at low frequencies with respect to their dry counterparts. The effect is smaller for the amyloid samples, especially the twisted fibrils.

The close similarity between the effect of hydration and that of supramolecular aggregation gives some clues toward the understanding of the reported results. In fact, the depression of low-frequency scattering and the apparent shift of the boson peak toward higher frequency as a consequence of hydration have previously been reported for other globular native proteins in which case it was assigned to strong hydrogen bonding between protein and hydration water which causes the damping of the low-frequency vibrational/librational motions responsible for the boson peak.[18] We propose that, in the case of fibrillar dry samples, the same damping mechanism could be

dx.doi.org/10.1021/jp412277y | J. Phys. Chem. B 2014, 118, 2913−2923

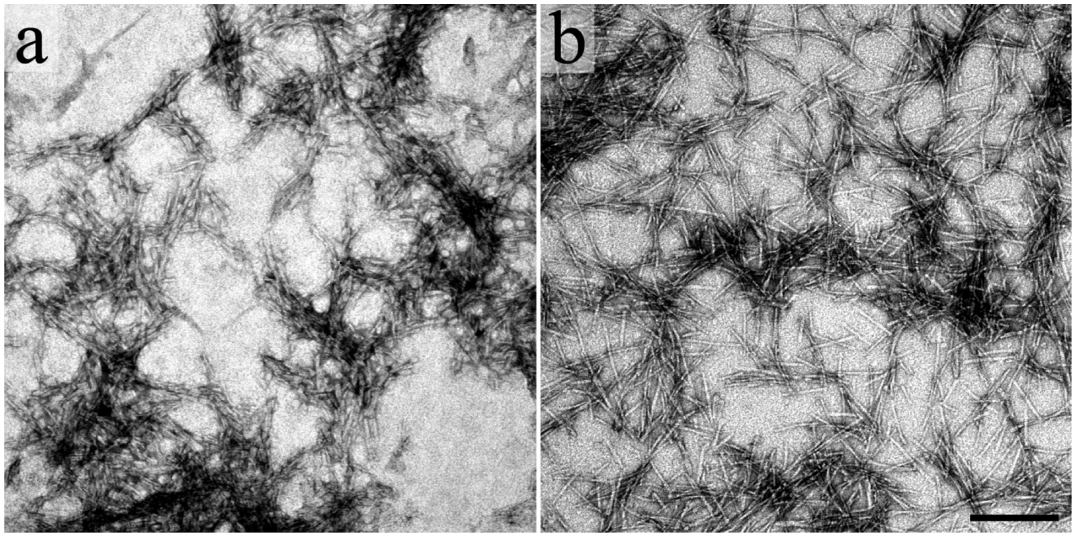

Figure 2. TEM measurements of twisted (a) and straight (b) fibril samples. Glucagon fibrils formed at low concentration exhibit a characteristic twist and consist of two or more protofilaments. The fibrils formed at high concentration consist of two protofilaments and are generally straight and unbranched. The bar represents 200 nm. The fibril morphology is conserved after freeze-drying, although the fibrils are fractured into shorter pieces in the process.

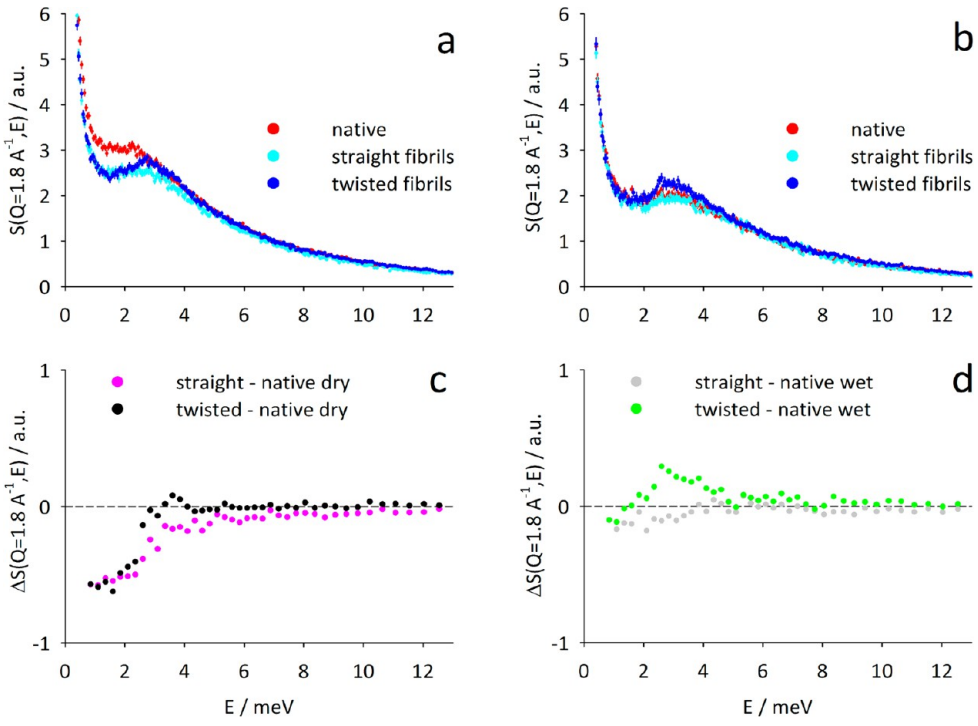

Figure 3. Inelastic neutron scattering spectra of glucagon powder samples: (a) dry samples; (b) hydrated samples (h = 0.15); (c) fibrils − native difference spectra relative to dry samples; (d) fibrils − native difference spectra relative to hydrated samples. Difference spectra in panels c and d are averaged every five data points to enhance the signal-to-noise ratio.

provided by the strong intermolecular protein−protein interactions promoted by the supramolecular aggregation. We stress that, in this picture, the depression of low-frequency scattering and the apparent high-frequency shift of the boson peak in wet protein powders and in fibrillar samples can be due to increased damping rather than to an alteration of the vibrational density of states (V-DOS).

In order to get a more quantitative understanding of the observed behavior, we analyzed the data using a model able to take into account the dissipative coupling with an external matrix and based on the mode-coupling theory.[23] As described in detail in the Materials and Methods section, the model takes into consideration a distribution of vibrational modes that are damped by the coupling with a dissipative bath. Note that both the distribution of modes (V-DOS) and the damping contribute to the shape and position of the boson peak, and also note that the tails at lower and higher energies with respect to the peak position are not due to quasi-elastic scattering from diffusive-like motions (which are well inside the elastic line at 150 K) but are fully accounted for by the model in its current

dx.doi.org/10.1021/jp412277y | J. Phys. Chem. B 2014, 118, 2913−2923

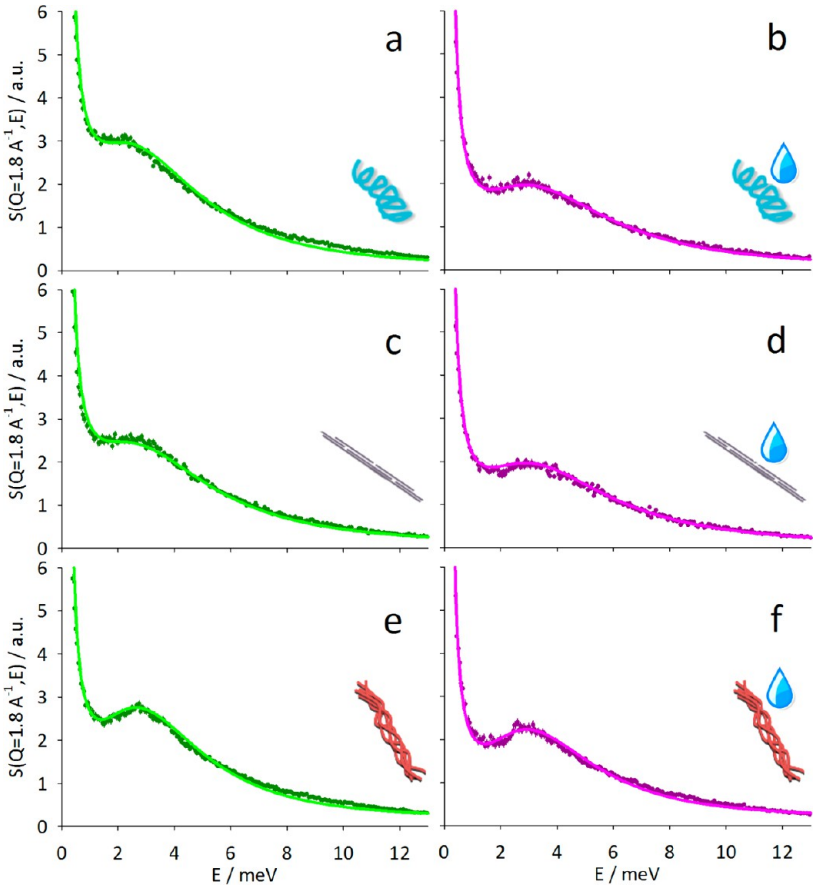

Figure 4. Inelastic neutron scattering data (points) and fitting curves (lines) of glucagon powder samples: (a, b) dry and hydrated native glucagon; (c, d) dry and hydrated straight fibrils; (e, f) dry and hydrated twisted fibrils.

Table 1. Fitting Parameters Obtained by the Analysis of Inelastic Spectra Shown in Figure 4 with the Model Discussed in the Materials and Methods Section[a]

	Θ [ln(meV)]	ρ [ln(meV)]	γ [meV^{-1}]	F	τ [meV^{-1}]
			dry		
native	1.25 ± 0.01	0.52 ± 0.01	1.376 ± 0.002	5.12 ± 0.01	17.4 ± 0.3
straight	1.14 ± 0.05	0.52 ± 0.01	1.259 ± 0.004	5.37 ± 0.03	15.8 ± 0.4
twisted	1.01 ± 0.01	0.54 ± 0.03	1.122 ± 0.002	5.45 ± 0.01	13.4 ± 0.1
			wet		
native	1.12 ± 0.01	0.48 ± 0.01	1.135 ± 0.001	5.71 ± 0.03	11.0 ± 0.8
straight	1.10 ± 0.02	0.50 ± 0.02	0.978 ± 0.004	5.48 ± 0.02	10.1 ± 0.2
twisted	1.02 ± 0.07	0.59 ± 0.02	0.94 ± 0.01	5.82 ± 0.02	10.8 ± 0.3

[a]Θ and ρ are the center and the width of the normal mode lognormal distribution, respectively; γ is the Newtonian friction; F and τ are the amplitude and the relaxation time of the Maxwell friction term, respectively.

form. The model provides results in excellent agreement with experimental data (Figure 4). The relevant best-fit parameters obtained from this analysis are reported in Table 1. (The global amplitude a and the constant background b are not reported because they do not determine the spectral shape and do not bear any physical information.) Results reported in Table 1 may appear counterintuitive at first sight, since they show that the observed blue shift of the boson peak is not due to a blue shift of the V-DOS (that actually appears to be red-shifted) but rather to increased damping. In order to clearly assess the reliability of our fitting procedure, we investigated the structure of the χ^2 surface as a function of the most relevant parameters Θ (the peak position of the V-DOS) and τ (the extent of damping). Typical contour plots are reported in Figure 5 for all glucagon states investigated. The plots clearly show that a single deep χ^2 minimum is found in a large range of variability of the two parameters and, most significantly, that no correlation exists between them. We therefore conclude that the results reported in Table 1 are not flawed by the fitting procedure.

Interestingly, even if the native, dry sample exhibits an overall spectrum red-shifted with respect to the hydrated one, as already observed for other proteins, its distribution of vibrational modes (see Table 1) is blue-shifted. This is fully in agreement with an increased stiffness accompanying an increase of β-structures in dry protein powders, as previously reported[19] (note that the secondary structure of hydrated native glucagon is predominantly composed by α-helix motifs). It also confirms the importance of the dissipation by water

dx.doi.org/10.1021/jp412277y | J. Phys. Chem. B 2014, 118, 2913−2923

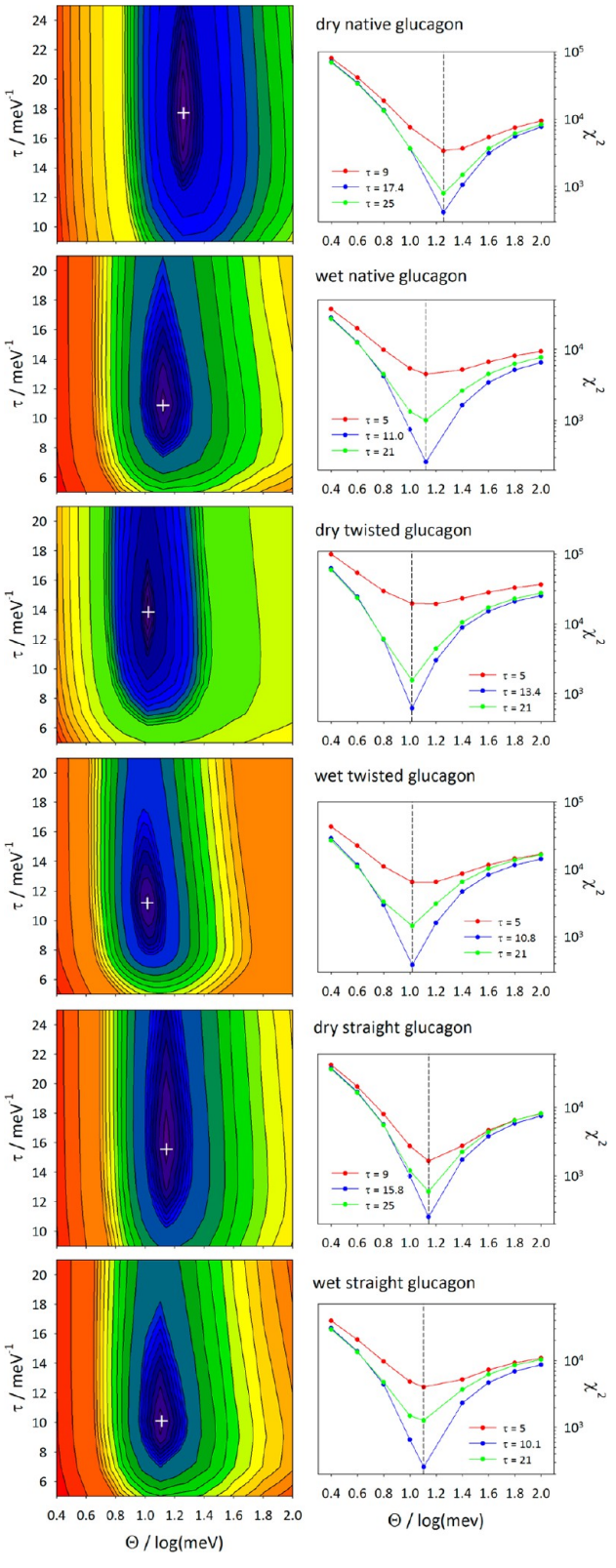

Figure 5. Results of the χ^2 function analysis. Left panels: contour plots of the χ^2 surface as a function of parameters Θ (peak position of the density of states) and τ (extent of damping). Right panels: χ^2 as a function of Θ at three selected values of τ; the vertical dashed lines correspond to the best value obtained with the fitting procedure. From top to bottom: dry native glucagon, hydrated native glucagon, dry twisted glucagon fibrils, hydrated twisted glucagon fibrils, dry straight glucagon fibrils, and hydrated straight glucagon fibrils.

matrix in determining the measured boson peak shape. The blue shift of the mode distribution as a consequence of dehydration is largely reduced in the fibril samples (see Table 1), as expected in view of their β-rich structures already in the hydrated state.

The analysis reported above sheds light on the effect of amyloid state on the boson peak and increases the understanding of the molecular mechanisms behind the observed behavior. Concerning the dry samples, both straight and twisted fibrillar states are characterized by a slightly red-shifted distribution of vibrational modes (lower Θ values) and by a markedly different viscoelastic behavior with respect to the native state. In fact, we observe a decrease of the elastic response (lower values of the Newtonian term γ) and an increase of the viscous term brought about by the simultaneous increase of the coupling with the dissipative bath (parameter F) and decrease of the relaxation time (parameter τ). All the above effects are enhanced in the twisted fibrils. The observed differences between the results obtained on the two fibril morphologies can be rationalized by considering their specific characteristics. The twisted fibrils are composed of several thin filaments closely packed together, thus producing a large interaction between protein surfaces, while the straight fibrils consist of fewer (1 or 2) protofilaments, so that protein surfaces are only partially involved in interfilament interactions. In summary, for dry samples, the amyloid state appears to be characterized by stiffer mechanical properties, as evidenced by a blue-shifted boson peak. This effect (which is slightly larger for twisted than for straight fibrils) is, however, not caused by a blue shift of the intrinsic V-DOS but rather by increased damping of low-frequency collective vibrations.

Concerning the hydrated samples, we note that they are in general characterized by increased damping (larger F and smaller τ values) and lowered elastic response (lower γ values) with respect to dry samples. This is compatible with the hypothesis by Doster and collaborators[18] stating that the hydration water is the main thing responsible for the suppression of low-frequency modes in the boson peak of hydrated protein powders through hydrogen bonding and electrostatic interactions with the polar side chains that hampers their low-frequency librational motions. Therefore, in the presence of hydration water, the damping of low-frequency motions (and thus the shape of the boson peak) is essentially dominated by water−protein interactions. The water matrix surrounding the proteins and interacting with them through electrostatic and hydrogen-bond interactions constitutes the main dissipative bath for protein vibrational modes. This "water-friction" mechanism acts essentially in the same way for native and fibrillar samples so that, differently from dry samples, the effect of amyloid aggregation is much smaller. In particular, as far as the damping parameters are concerned, we observe small effects, partly compensating each other. As an example, for straight fibrils, the smaller value of parameter F (amplitude of the Maxwell friction) is partly compensated by the smaller relaxation time. On the other hand, fibrillar samples seem to be characterized by a smaller Newtonian friction (parameter γ). Concerning the distribution of vibrational states, the effect of amyloid conformation is more clear: the V-DOS appears to be wider and red-shifted, the effect being almost within the error for straight fibrils and more pronounced for twisted fibrils. This reflects the fact that, as shown in Figure 3b, the inelastic spectra of native polypeptide and of straight fibrils are hardly distinguishable, while that of twisted fibrils is clearly

dx.doi.org/10.1021/jp412277y | J. Phys. Chem. B 2014, 118, 2913−2923

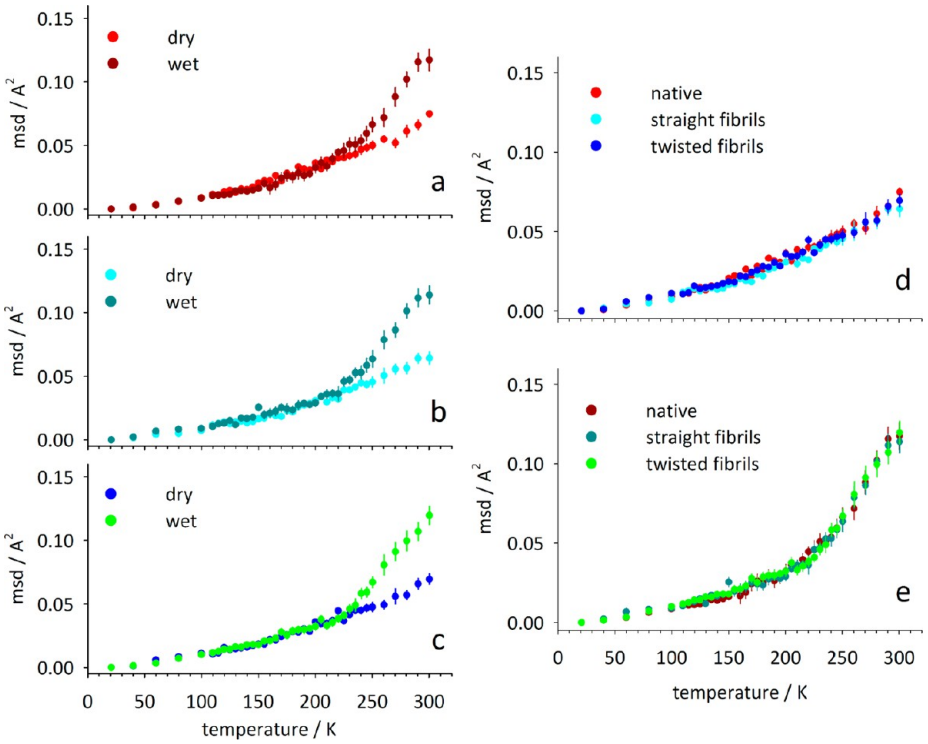

Figure 6. Temperature dependence of total mean square displacements of nonexchangeable hydrogen atoms in glucagon samples. Left panels: native glucagon (a), straight glucagon fibrils (b), and twisted glucagon fibrils (c). Right panels: the same data as in the left panels grouped for hydration conditions, i.e., dry (d) and hydrated (e) samples.

red-shifted. Note that, in the case of hydrated twisted fibrils, the red shift of the boson peak is indeed caused by a red shift of the V-DOS. This suggests that structural modifications occurring in the twisted fibrils not only modify intermolecular interactions (as evidenced by the increased damping observed in the dry samples) but also affect the intrinsic V-DOS and the mechanical properties, as shown on the basis of simple mechanics models like, e.g., the Euler–Bernouilli beam model.[40] A dependence of amyloid mechanical properties on fibril structural heterogeneity and on polymorphism has been observed previously (see Sweers et al.[41] and references therein) with out-of-equilibrium single molecule techniques. Here we show that probing equilibrium collective vibrations reveals a similar behavior. On the basis of our results, the hydrated twisted glucagon fibrils are expected to be softer than the hydrated straight ones. A validation of this hypothesis through experiments or computer simulations would be highly desirable. We stress, however, that computer simulations should take into account the damping of vibrational modes due to protein–protein and/or protein–water interactions.

Elastic Neutron Scattering. A different possible explanation of the observed effect, namely, the apparent hydration-like behavior of dry straight and twisted fibrils, could be the presence of a non-negligible amount of water molecules trapped in the cavities formed during the formation of the aggregated supramolecular structure and not removed even after thermogravimetric analysis. This possibility was checked by performing elastic neutron scattering experiments on the same samples. Elastic scattering experiments on deuterated powders enables measurements of the temperature dependence of the msd of nonexchangeable hydrogen atoms[42] and thus return relevant information concerning equilibrium protein fluctuations[43] and on how they are affected by the amyloid state and protein–water interactions. In particular, it has been shown that the msd measured above the temperature of the so-called protein dynamical transition (defined as the steep increase of msd activated in hydrated samples at about 220 K[44−46]) depend markedly upon the sample hydration.

The msd of protein hydrogen atoms were calculated from elastic data as detailed in Materials and Methods, and their temperature dependence is reported in Figure 6. It is clearly seen that for both the dry and hydrated samples the aggregation state does not modify the onset temperature of the protein dynamical transition (Figure 6a–c) nor the msd absolute amplitudes in the whole temperature range investigated (Figure 5d,e). This confirms that in our samples no difference in water content is detected and it is therefore possible to exclude that relevant quantities of water are trapped in the fibril structure. Note that elastic data—showing no effect of glucagon amyloid state on the high temperature anharmonic dynamics—are not in conflict with inelastic data on the boson peak measured at 150 K. Indeed, the effects measured on the boson peak (V-DOS shifts and increased damping) refer to the low frequency harmonic vibrational dynamics and are too small to be detected in the linear low-temperature dependence of msd. On the other hand, the higher temperature msd are mainly determined by activated anharmonic motions, like, e.g., methyl group rotations[47−50] and hydration water related jumps between conformational substates,[42,46,45,51] and are therefore almost insensitive to vibrational dynamics.

It is interesting to compare the present elastic data with data previously obtained with the same technique on Concanavalin A (Con A) amyloid fibrils.[38] Con A is a 26 kDa globular protein dominated by β-sheet structures in the native state. It readily forms fibrils via a non-nucleated mechanism involving the formation of intermolecular β-sheets.[52,53] The results of that

dx.doi.org/10.1021/jp412277y | J. Phys. Chem. B 2014, 118, 2913–2923

study indicated that Con A amyloid fibrils (in contrast to the glucagon fibrils investigated here) show enhanced atomic fluctuations with respect to the native state. The behavior of Con A fibrils was attributed to the structural constraints leading to amyloid formation which brings the protein to expose side chains to the fibril surface, thus allowing a plasticizing interaction with hydration water. That mechanism (i.e., the enhancement of atomic fluctuations due to a change in protein side chain exposure during the fibril formation) is coherent with the present results on glucagon fibrils. Indeed, in a globular protein like Con A, a number of side chains usually buried in the internal core of the protein are forced to be exposed to the solvent in the fibril structure, thus accounting for the observed msd enhancement. In the case of a small, flexible peptide such as glucagon, it is not possible to the same extent to define a group of internal side chains, and solvent exposure of side chains upon fibril formation thus occurs to a much lesser extent with similar negligent effect on the amplitude of atomic fluctuations.

CONCLUSIONS

In this work, inelastic neutron scattering was used to probe the effect of the amyloid fibril state on the boson peak of glucagon. To our knowledge, this is the first time the neutron inelastic spectrum of a peptide fixed in specific fibril states has been studied. We found that the molecular structure and organization of glucagon fibrils affect the shape and position of the boson peak, with the effect being dependent on the sample hydration state and on the fibrillar morphology. Using a model for a viscoelastic system of damped oscillators, we described the observed effects in terms of changes in the distribution of vibrational modes and in terms of the dissipative mechanism provided by water−protein and protein−protein interactions. Our analysis also confirms that the observed red shift of the boson peak in native proteins upon drying is largely determined by the change of the dissipative mechanism provided by water.

It was recently suggested that water−protein interaction is a key factor in determining mechanics and energetics of fibrils.[54,55,38] In particular, water is an important player in the definition of the protein energy landscape, which defines the conformational path toward the aggregated state. D. Thirumalai and collaborators showed[55] that water-mediated interactions drive oligomer formation in Aβ peptides and provided scenarios for the role water plays in inducing polymorphic amyloid structures. Our results demonstrate that, in the presence of water, water−protein interactions (or, in general, water-mediated interactions), essentially determine the viscoelastic properties of the glucagon peptide, regardless of protein conformation and aggregate polymorphism. However, when water is removed, the role of protein−protein interactions is highlighted and in this case the specific interactions necessary for the proteins to form the supramolecular amyloid assemblies dominate the viscoelastic properties. These protein−protein interactions, our data shows, depend on the fibril morphology. The interplay between protein−protein and protein−water interactions during fibrillation is still poorly understood, but our evidence that a water-like dissipation mechanism is present in the dry glucagon fibrils suggests that the energetics of water exclusion during fibril growth is compensated for by the formation of an extended pattern of interfacial amyloid interactions.

Our results also indicate that the damping of low-frequency collective vibrations is the main mechanism responsible for the observed effects. Therefore, we suggest that any study of nanomechanical properties of amyloids (either experimental or simulative) should take into proper consideration the hydration state and morphology of the sample and the presence of dissipative mechanisms. It is also noteworthy that, in twisted glucagon fibrils, a red shift of the distribution of low-frequency vibrational states is observed, suggesting softer mechanical properties in this species. This result prompts for further experimental and theoretical/computational investigations on the morphology dependence of fibril nanomechanical properties.

ASSOCIATED CONTENT

Supporting Information

Inelastic neutron scattering spectra of dry and hydrated glucagon samples and relative dry-hydrated difference spectra. This material is available free of charge via the Internet at http://pubs.acs.org.

AUTHOR INFORMATION

Corresponding Author

*E-mail: giorgio.schiro@ibs.fr.

Present Address

$^{\perp}$(G.S.) CNRS - Institut de Biologie Structurale, Grenoble, France.

Notes

The authors declare no competing financial interest.

ACKNOWLEDGMENTS

The authors acknowledge the Institut Laue-Langevin (Grenoble, France) for beamtime allocation at IN6 and IN13 stations, Novo Nordisk (Copenhagen, Denmark) for kindly providing native glucagon samples, Ane Margrethe Blom (Novo Nordisk) for the TEM measurements, and Federica Piccirilli (University of Palermo) for the careful reading of the manuscript.

REFERENCES

(1) Rochet, J. C.; Lansbury, P. T., Jr. Amyloid Fibrillogenesis: Themes And Variations. *Curr. Opin. Struct. Biol.* **2000**, *10*, 60.

(2) Frokjaer, F.; Otzen, D. E. Protein Drug Stability: A Formulation Challenge. *Nat. Rev. Drug Discovery* **2005**, *4*, 298.

(3) Otzen, D.; Nielsen, P. H. We Find Them Here, We Find Them There: Functional Bacterial Amyloid. *Cell. Mol. Life Sci.* **2008**, *65*, 910.

(4) Knowles, T. P. J.; Buehler, M. J. Nanomechanics Of Functional And Pathological Amyloid Materials. *Nat. Nanotechnol.* **2011**, *6*, 469.

(5) Scheibel, T.; Parthasarathy, R.; Sawicki, G.; Lin, X.-M.; Jaeger, H.; Lindquist, S. L. Conducting Nanowires Built By Controlled Self-Assembly Of Amyloid Fibers And Selective Metal Deposition. *Proc. Natl. Acad. Sci. U.S.A.* **2003**, *100*, 4527.

(6) Smith, J. F.; Knowles, T. P. J.; Dobson, C. M.; Macphee, C. E.; Welland, M. E. Characterization Of The Nanoscale Properties Of Individual Amyloid Fibrils. *Proc. Natl. Acad. Sci. U.S.A.* **2006**, *103*, 15806.

(7) Mankar, S.; Anoop, A.; Sen, S.; Maji, S. K. Nanomaterials: Amyloids Reflect Their Brighter Side. *Nano Rev.* **2011**, *2*, 6032.

(8) Pedersen, J. S.; Andersen, C. B.; Otzen, D. E. Amyloid Structure−One But Not The Same: The Many Levels Of Fibrillar Polymorphism. *FEBS J.* **2010**, *277*, 4591.

(9) Petkova, A. T.; Leapman, R. D.; Guo, Z.; Yau, W. M.; Mattson, M. P.; Tycko, R. Self-Propagating, Molecular-Level Polymorphism In Alzheimer's ß-Amyloid Fibrils. *Science* **2005**, *307*, 262.

(10) Fändrich, M.; Meinhardt, J.; Grigorieff, N. Structural Polymorphism Of Alzheimer Aβ And Other Amyloid Fibrils. *Prion* **2009**, *3*, 89.
(11) Knowles, T. P. J.; Shu, W.; Devlin, G. L.; Meehan, S.; Auer, S.; Dobson, C. M.; Welland, M. E. Kinetics And Thermodynamics Of Amyloid Formation From Direct Measurements Of Fluctuations In Fibril Mass. *Proc. Natl. Acad. Sci. U.S.A.* **2007**, *104*, 10016.
(12) Cusack, S.; Doster, W. Temperature Dependence Of The Low Frequency Dynamics Of Myoglobin. Measurement Of The Vibrational Frequency Distribution By Inelastic Neutron Scattering. *Biophys. J.* **1990**, *58*, 243.
(13) Kurkal-Siebert, V.; Smith, J. Low-Temperature Protein Dynamics: A Simulation Analysis Of Interprotein Vibrations And The Boson Peak At 150 K. *J. Am. Chem. Soc.* **2006**, *128*, 2356.
(14) Bizzarri, A. R.; Paciaroni, A.; Arcangeli, C.; Cannistraro, S. Low-Frequency Vibrational Modes In Proteins: A Neutron Scattering Investigation. *Eur. Biophys. J.* **2001**, *30*, 443.
(15) De Francesco, A.; Marconi, M.; Cinelli, S.; Onori, G.; Paciaroni, A. Picosecond Internal Dynamics Of Lysozyme As Affected By Thermal Unfolding In Nonaqueous Environment. *Biophys. J.* **2004**, *86*, 480.
(16) Diehl, M.; Doster, W.; Petry, W.; Schober, H. Water-Coupled Low-Frequency Modes Of Myoglobin And Lysozyme Observed By Inelastic Neutron Scattering. *Biophys. J.* **1997**, *73*, 2726.
(17) Tarek, M.; Tobias, D. J. Effects Of Solvent Damping On Side Chain And Backbone Contributions To The Protein Boson Peak. *J. Chem. Phys.* **2001**, *115*, 1607.
(18) Leyser, H.; Doster, W.; Diehl, M. Far-Infrared Emission By Boson Peak Vibrations In A Globular Protein. *Phys. Rev. Lett.* **1999**, *82*, 2987.
(19) Griebenow, K.; Klibanow, A. M. Lyophilization-Induced Reversible Changes In The Secondary Structure Of Proteins. *Proc. Natl. Acad. Sci. U.S.A.* **1995**, *92*, 10969.
(20) T. Ackbarow, T.; Chen, X.; Keten, S.; Buehler, M. J. Hierarchies, Multiple Energy Barriers, And Robustness Govern The Fracture Mechanics Of A-Helical And B-Sheet Protein Domains. *Proc. Natl. Acad. Sci. U.S.A.* **2007**, *104*, 16410.
(21) Perticaroli, S.; Nickels, J. D.; O'Neill, H.; Zhang, Q.; Ehlers, G.; Sokolov, A. P. Secondary Structure And Rigidity In Model Proteins. *Soft Matter* **2013**, *9*, 9548.
(22) Gaspar, A.; Appavou, M. S.; Busch, S.; Unruh, T.; Doster, W. Dynamics Of Well-Folded And Natively Disordered Proteins In Solution: A Time-Of-Flight Neutron Scattering Study. *Eur. Biophys. J.* **2008**, *37*, 573.
(23) Goetze, W.; Sjogren, L. Comments On The Mode Coupling Theory For Structural Relaxation. *Chem. Phys.* **1996**, *212*, 47.
(24) Chou, K. C. Biological Functions Of Low-Frequency Vibrations (Phonons). III. Helical Structures And Microenvironment. *Biophys. J.* **1984**, *45*, 881.
(25) Schiro, G.; Caronna, C.; Natali, F.; Koza, M. M.; Cupane, A. The "Protein Dynamical Transition" Does Not Require The Protein Polypeptide Chain. *J. Phys. Chem. Lett.* **2011**, *2*, 2275.
(26) Suezaki, Y.; Gō, N. Breathing Mode Of Conformational Fluctuations In Globular Proteins. *Int. J. Pept. Protein Res.* **1975**, *7*, 333.
(27) Estall, J. L.; Drucker, D. J. Glucagon And Glucagon-Like Peptide Receptors As Drug Targets. *Curr. Pharm. Des.* **2012**, *12*, 1731.
(28) Gratzer, W. B.; Beaven, G. H.; Rattle, H. W.; Bradbury, E. M. A Conformational Study Of Glucagon. *Eur. J. Biochem.* **1968**, *3*, 276.
(29) De Jong, K. L.; Incledon, B.; Yip, C. M.; Defelippis, M. R. Amyloid Fibrils Of Glucagon Characterized By High-Resolution Atomic Force Microscopy. *Biophys. J.* **2006**, *91*, 1905.
(30) Andersen, C. B.; Yagi, H.; Manno, M.; Martorana, V.; Ban, T.; Christiansen, G.; Otzen, D. E.; Goto, Y.; Rischel, C. Branching In Amyloid Fibril Growth. *Biophys. J.* **2009**, *96*, 1529.
(31) Macchi, F.; Hoffmann, S. V.; Carlsen, M.; Vad, B.; Imparato, A.; Rischel, C.; Otzen, D. E. Mechanical Stress Affects Glucagon Fibrillation Kinetics And Fibril Structure. *Langmuir* **2011**, *27*, 12539.
(32) Andersen, C. B.; Otzen, D.; Christiansen, G.; Rischel, C. Glucagon Amyloid-Like Fibril Morphology Is Selected Via Morphology-Dependent Growth Inhibition. *Biochemistry* **2007**, *46*, 7314.
(33) Andersen, C. B.; Hicks, M. R.; Vetri, V.; Vandahl, B.; Rahbek-Nielsen, H.; Thøgersen, H.; Thøgersen, I. B.; Enghild, J. J.; Serpell, L. C.; Rischel, C.; Otzen, D. E. Glucagon Fibril Polymorphism Reflects Differences In Protofilament Backbone Structure. *J. Mol. Biol.* **2010**, *397*, 932.
(34) Pedersen, J. S.; Dikov, D.; Flink, J. L.; Hjuler, H. A.; Christiansen, G.; Otzen, D. E. The Changing Face Of Glucagon Fibrillation: Structural Polymorphism And Conformational Imprinting. *J. Mol. Biol.* **2006**, *355*, 501.
(35) Jeppesen, M. D.; Hein, K.; Nissen, P.; Westh, P.; Otzen, D. E. A Thermodynamic Analysis Of Fibrillar Polymorphism. *Biophys. Chem.* **2010**, *149*, 40.
(36) Malinovsky, V. K.; Novikov, V. N.; Sokolov, A. P. Log-Normal Spectrum Of Low-Energy Vibrational Excitations In Glasses. *Phys. Lett. A* **1991**, *153*, 63.
(37) Gabel, F.; Bicout, D.; Lehnert, U.; Tehei, M.; Weik, M.; Zaccai, G. Protein Dynamics Studied By Neutron Scattering. *Q. Rev. Biophys.* **2002**, *35*, 327.
(38) Schirò, G.; Vetri, V.; Frick, B.; Militello, V.; Leone, M.; Cupane, A. Neutron Scattering Reveals Enhanced Protein Dynamics In Concanavalin A Amyloid Fibrils. *J. Phys. Chem. Lett.* **2012**, *3*, 992.
(39) Xu, Z.; Paparcone, R.; Buehler, M. J. Alzheimer's Aβ(1−40) Amyloid Fibrils Feature Size-Dependent Mechanical Properties. *Biophys. J.* **2010**, *98*, 2053.
(40) Yoon, G.; Kwak, J.; Kim, J. I.; Na, S.; Eom, K. Mechanical Characterization Of Amyloid Fibrils Using Coarse−Grained Normal Mode Analysis. *Adv. Funct. Mater.* **2011**, *21*, 3454.
(41) Sweers, K. K. M.; Bennink, M. L.; Subramaniam, V. Nanomechanical Properties Of Single Amyloid Fibrils. *J. Phys.: Condens. Matter* **2012**, *24*, 243101.
(42) Doster, W.; Cusack, S.; Petry, W. Dynamical Transition Of Myoglobin Revealed By Inelastic Neutron Scattering. *Nature* **1989**, *337*, 754.
(43) Zaccai, G. How Soft Is A Protein? A Protein Dynamics Force Constant Measured By Neutron Scattering. *Science* **2000**, *288*, 1604.
(44) Roh, J. H.; Briber, R. M.; Damjanovic, A.; Thirumalai, D.; Woodson, S. A.; Sokolov, A. P. Dynamics Of Trna At Different Levels Of Hydration. *Biophys. J.* **2009**, *96*, 2755.
(45) Wood, K.; Frölich, A.; Paciaroni, A.; Moulin, M.; Härtlein, M.; Zaccai, G.; Tobias, D. J.; Weik, M. Coincidence Of Dynamical Transitions In A Soluble Protein And Its Hydration Water: Direct Measurements By Neutron Scattering And MD Simulations. *J. Am. Chem. Soc.* **2008**, *130*, 4586.
(46) Schirò, G.; Natali, F.; Cupane, A. Physical Origin Of Anharmonic Dynamics In Proteins: New Insights From Resolution-Dependent Neutron Scattering On Homomeric Polypeptides. *Phys. Rev. Lett.* **2012**, *109*, 10215.
(47) Roh, J. H.; Novikov, V. N.; Gregory, R. B.; Curtis, J. E.; Chowdhuri, Z.; Sokolov, A. P. Onsets Of Anharmonicity In Protein Dynamics. *Phys. Rev. Lett.* **2005**, *95*, 038101.
(48) Caliskan, G.; Briber, R. M; Thirumalai, D.; Garcia-Sakai, V.; Woodson, S. A.; Sokolov, A. P. Dynamic Transition In Trna Is Solvent Induced. *J. Am. Chem. Soc.* **2006**, *128*, 32.
(49) Schirò, G.; Caronna, C.; Natali, F.; Cupane, A. Direct Evidence Of The Amino Acid Side Chain And Backbone Contributions To Protein Anharmonicity. *J. Am. Chem. Soc.* **2010**, *132*, 1371.
(50) Wood, K.; Tobias, D. J.; Kessler, B.; Gabel, F.; Oesterhelt, D.; Mulder, F. A.; Zaccai, G.; Weik, M. The Low-Temperature Inflection Observed In Neutron Scattering Measurements Of Proteins Is Due To Methyl Rotation: Direct Evidence Using Isotope Labeling And Molecular Dynamics Simulations. *J. Am. Chem. Soc.* **2010**, *132*, 4990.
(51) Schirò, G. Anharmonic Onsets In Polypeptides Revealed By Neutron Scattering: Experimental Evidences And Quantitative Description Of Energy Resolution Dependence. *Biophys Chem.* **2013**, *180−181*, 29.

(52) Vetri, V.; Canale, C.; Relini, A.; Librizzi, F.; Militello, V.; Gliozzi, A.; Leone, M. Amyloid Fibrils Formation And Amorphous Aggregation In Concanavalin A. *Biophys. Chem.* **2007**, *125*, 184.
(53) Carrotta, R.; Vetri, V.; Librizzi, F.; Martorana, V.; Militello, V.; Leone, M. Amyloid Fibrils Formation Of Concanavalin A At Basic Ph. *J. Phys. Chem. B* **2011**, *115*, 2691.
(54) Abou Neel, E. A.; Cheema, U.; Knowles, J. C.; Brown, R. A.; Nazhat, S. N. Use Of Multiple Unconfined Compression For Control Of Collagen Gel Scaffold Density And Mechanical Properties. *Soft Matter* **2006**, *2*, 986.
(55) Thirumalai, D.; Reddy, G.; Straub, J. Role Of Water In Protein Aggregation And Amyloid Polymorphism. *Acc. Chem. Res.* **2012**, *45*, 83.